Author Manuscript

Author Manuscript

Author Manuscript

Author Manuscript

HHS Public Access

Author manuscript

J Immunol. Author manuscript; available in PMC 2015 April 20.

Published in final edited form as:

J Immunol. 2007 April 15; 178(8): 5227–5236.

CD8+ T Cell Dysfunction and Increase in Murine Gammaherpesvirus Latent Viral Burden in the Absence of 4-1BB Ligand[1]

Shinichiro Fuse[*], **Sarah Bellfy**[*], **Hideo Yagita**[†], and **Edward J. Usherwood**[2,*]

[*]Department of Microbiology and Immunology, Dartmouth Medical School, Lebanon, NH 03756

[†]Department of Immunology, Juntendo University School of Medicine, Tokyo, Japan

Abstract

Studies of costimulatory receptors belonging to the TNFR family have revealed their diverse roles in affecting different stages of the T cell response. The 4-1BB ligand (4-1BBL)/4-1BB pathway has emerged as a receptor-ligand pair that impacts not the initial priming, but later phases of the T cell response, such as sustaining clonal expansion and survival, maintaining memory $CD8^+$ T cells, and supporting secondary expansion upon Ag challenge. Although the role of this costimulatory pathway in $CD8^+$ T cell responses to acute viral infections has been well-studied, its role in controlling chronic viral infections in vivo is not known to date. Using the murine gammaherpesvirus-68 (MHV-68) model, we show that 4-1BBL-deficient mice lack control of MHV-68 during latency and show significantly increased latent viral loads. In contrast to acute influenza infection, the numbers of MHV-68-specific memory $CD8^+$ T cells were maintained during latency. However, the virus-specific $CD8^+$ T cells showed defects in function, including decreased cytolytic function and impaired secondary expansion. Thus, 4-1BBL deficiency significantly affects the function, but not the number, of virus-specific $CD8^+$ T cells during gammaherpesvirus latency, and its absence results in an increased viral burden. Our study suggests that the 4-1BB costimulatory pathway plays an important role in controlling chronic viral infections.

Costimulatory signals provide secondary signals to T cells along with the TCR signal and are required for generating and maintaining responses of full capacity to viral infections (1–4). The 4-1BB ligand (4-1BBL)[3]/4-1BB receptor-ligand pair belongs to the TNF-TNFR family. 4-1BBL is mainly expressed on activated APCs such as dendritic cells (DCs), macrophages, and B cells. Its expression can also be induced on nonimmune cells during

[1]This work was supported by National Institutes of Health Grant CA103642.

Copyright © 2007 by The American Association of Immunologists, Inc.

[2]Address correspondence and reprint requests to Dr. Edward J. Usherwood, Department of Microbiology and Immunology, Dartmouth Medical School, 1 Medical Center Drive, Lebanon, NH 03756. edward.j.usherwood@dartmouth.edu.

Disclosures

The authors have no financial conflict of interest.

[3]Abbreviations used in this paper: 4-1BBL, 4-1BB ligand; DC, dendritic cell; BM-MC, bone marrow-derived mast cell; LCMV, lymphocytic choriomeningitis virus; MHV-68, murine gammaherpesvirus-68; i.n., intranasal; QF, quantitative fluorescent; CMC, carboxymethyl-cellulose; CTO, CellTracker Orange; MLN, mesenteric lymph node; VSV, vesicular stomatitis virus.

Author Manuscript Author Manuscript Author Manuscript Author Manuscript

inflammatory conditions (4) and bone marrow-derived mast cells (BM-MCs) upon activation (5). Its receptor, 4-1BB, is expressed on activated $CD4^+$ and $CD8^+$ T cells, as well as a subset of splenic DCs, and activated BM-MCs (4, 5). Costimulation through the 4-1BBL-4-1BB pathway provides cell proliferation and survival signals to T cells (6–8) and can augment protection in tumor challenge models (9–12). In contrast, 4-1BB stimulation can result in the triggering of suppressive T cell responses in certain models by diverse mechanisms (13–21).

In in vivo viral infection models, 4-1BB costimulation has been shown to affect mainly the antiviral $CD8^+$ T cell response (22–31). Interestingly, studies by Bertram et al. (22, 23) have revealed a specific role for 4-1BB costimulation in the maintenance of memory $CD8^+$ T cells and recall responses during influenza infection. Furthermore, protection from lymphocytic choriomeningitis virus (LCMV) after peptide vaccination was shown to require 4-1BB costimulation (31). The role for 4-1BB costimulation in the long-term $CD8^+$ T cell response brings up an interesting question: during a chronic infection where the virus (Ag) persists, is the 4-1BBL/4-1BB pathway required for the maintenance of the $CD8^+$ T cell response? If so, does the host lose control of virus replication in the absence of this pathway?

Infection by herpesviruses results in viral persistence which lasts throughout the lifetime of the animal. During this lifelong infection, the virus is kept under control by the immune system and dysfunctions in the immune system can result in reactivation of the virus leading to disease. Reactivation of human herpesviruses, such as HSV, CMV, and EBV or Kaposi's sarcoma-associated herpesvirus (HHV-8), has been reported in HIV-infected patients with progressive AIDS, or immunosuppressed individuals undergoing transplantation (32–35). The understanding of mechanisms regarding how the immune system prevents viral reactivation during the latent infection is not completely understood and will provide important information for the development of therapies to prevent or treat viral recrudescence.

The murine gammaherpesvirus-68 (MHV-68) is the only small animal model available for studying gammaherpesvirus pathogenesis and immunity in vivo. Infection by MHV-68 results in acute replication in the lungs for the first 2 wk which is controlled by $CD4^+$ and $CD8^+$ T cells (36, 37), and causes a lifelong latent infection in B cells, macrophages, DCs, and lung epithelial cells (38 – 41). Immune surveillance during the latent phase is maintained by $CD4^+$, $CD8^+$ T cells, and Abs (37, 39, 42, 43). Despite this knowledge, we currently lack understanding of detailed molecular mechanisms of how optimal T and B cell responses are generated and maintained during the MHV-68-specific response.

Several costimulatory pathways have been shown to mediate key signals in antiviral immunity against MHV-68. The CD40L-CD40 pathway is essential for long-term immunological control of latent infection (44, 45). The CD80/CD86-CD28 pathway has a significant impact in the antiviral humoral (42, 46), and cellular (46, 47) responses, and low levels of viral reactivation during latency is observed in the lungs of $CD80/CD86^{-/-}$ mice (47, 48). In this study, we investigated the role of the 4-1BBL-4-1BB pathway in immune surveillance of MHV-68 infection. 4-1BB expression was observed on virus-specific

Author Manuscript Author Manuscript Author Manuscript Author Manuscript

effector $CD8^+$ T cells, but not on memory cells. 4-1BBL$^{-/-}$ mice were capable of controlling acute viral replication and no sign of viral replication was observed during latency. However, the latent viral load was significantly increased in the lungs and spleens of 4-1BBL$^{-/-}$ mice. Although the number of virus-specific $CD8^+$ T cells was not affected, the cytotoxicity of virus-specific memory $CD8^+$ T cells and recall responses to viral challenge were significantly impaired by the absence of 4-1BBL. These results reveal a specific role for 4-1BB costimulation in the maintenance of antiviral $CD8^+$ T cell function during latent MHV-68 infection and thus its requirement for immune surveillance of the infection.

Materials and Methods

Mice, virus, and reagents

MHV-68 virus (clone G2.4) was originally obtained from Prof. A. A. Nash (University of Edinburgh, Edinburgh, U.K.). Virus was propagated and titered as previously described (49). A recombinant vaccinia virus expressing the $ORF61_{524–531}/K^b$ or the $ORF6_{487–495}/D^b$ epitope of MHV-68 (rVV-ORF61 and rVV-ORF6, respectively) was obtained from Dr. P. Doherty (St. Jude Children's Research Hospital, Memphis, TN) (50). For MHV-68 infections, mice were infected intranasally (i.n.) with 400 PFU under anesthesia with 2,2,2-tribromoethanol. For vaccinia virus challenge, mice were given 10^6 PFU recombinant vaccinia virus i.p., unless stated otherwise.

C57BL/6 and congenic B6-Ly5.2-Cr (which are Ly5.1/CD45.1$^+$) mice were purchased from the National Cancer Institute (Bethesda, MD). 4-1BBL$^{-/-}$ mice on the C57BL/6 background were obtained from Dr. W. Green (Dartmouth Medical School, Lebanon, NH), and bred in the Dartmouth-Hitchcock Medical Center mouse facility. Permission was obtained from Amgen to use the mice for the study. The Animal Care and Use Program of Dartmouth College approved all animal experiments.

Tissue preparation

Single-cell suspensions of spleens and mediastinal lymph nodes were prepared by passing through cell strainers. Lungs were injected with 2 ml of MEM containing 417.5 μg/ml Liberase CI and 200 μg/ml DNase I (both obtained from Roche), minced with scissors, then incubated for 30 min at 37°C, and passed through cell strainers. Suspensions were resuspended in 80% isotonic Percoll and subsequently overlaid with 40% isotonic Percoll. Samples were then centrifuged at 400 × g for 25 min at 4°C and the cells at the 80%/40% interface were collected, washed, and counted.

Quantitative PCR for viral transcripts

Latent viral DNA was quantified by quantitative fluorescent (QF)-PCR for the *ORF50* gene as previously described (51).

The standard plaque assay and in vitro amplification

Infectious virus titers in the lungs were determined by standard plaque assays as previously described (49). The in vitro-amplified plaque assay has been described previously (47). Briefly, to allow amplification of viral titers, a 1/10 dilution of lung homogenates was added

Author Manuscript Author Manuscript Author Manuscript Author Manuscript

to NIH3T3 cell monolayers in duplicate, and were cultured for 6 days without the addition of carboxymethyl-cellulose (CMC). An additional 1 ml of medium was added at day 2. At day 6, cells and supernatants were collected, freeze-thawed to release the virus replicating inside the cells, spun down, and virus titers in the supernatants were measured using a standard plaque assay.

MHC/peptide tetramer, Ab staining, and flow cytometric analysis

MHC/peptide tetramers for the MHV-68 epitopes, $ORF61_{524–531}$(TSINFVKI)/K^b, $ORF6_{487–495}$(AGPHNDMEI)/D^b, or the vaccinia virus epitope $B8R_{20–27}$(TSYKFESV)/K^b, which were conjugated to allophycocyanin, were obtained from the National Institutes of Health Tetramer Core Facility (Emory University, Atlanta, GA). Cells were stained for 1 h at room temperature in the dark as previously described (51). Cells were further stained with PerCP-conjugated anti-CD8α (clone 53-6.7), and Abs against the following surface markers; FITC-conjugated anti-CD44 (IM7), FITC-conjugated anti-CD62L (MEL-14), FITC-conjugated anti-CD27 (LG.7F9), FITC-conjugated anti-CD69 (H1.2F3), PE-conjugated anti-CD127 (A7R34), PE-conjugated anti-CD122 (SH4), PE-conjugated anti-CD25 (PC61), or the corresponding isotype control Abs. To assess 4-1BB expression, cells were stained with anti-4-1BB (17B5) or control Ab. Staining and analysis was done as previously described (51).

In vivo cytotoxicity assay

Naive C57BL/6 splenocytes were pulsed with 1 μg/ml of the $ORF61_{524–531}$, $ORF6_{487–495}$ peptide, or no peptide and were labeled with 2.5 μM, 0.25 μM CFSE (Molecular Probes), or 10 μM CellTracker Orange (CTO; Molecular Probes), respectively. Cells were mixed at a 1:1:1 ratio, and ~2×10^7 cells were injected i.v. One day later, mice were sacrificed and collected spleen cell suspensions were incubated with 20 μg/ml 7-aminoactinomycin D (7-AAD; Sigma-Aldrich) for 15 min at room temperature in the dark to label dead cells. Cells were analyzed by flow cytometry and specific lysis was calculated using the formulas: ratio = (number CFSE/number CTO); percentage of specific lysis = (1 − (ratio of naive/ratio of infected) × 100).

Intracellular cytokine staining and degranulation assay

Splenocytes were incubated with 1 or 0.01 μg/ml of the appropriate peptide plus 10 U/ml IL-2 and 10 μg/ml brefeldin A in complete medium at 37°C for 5 h. Cells were stained with anti-CD8 and anti-CD44 Ab, then fixed and rendered permeable before staining with allophycocyanin-conjugated anti-IFN-γ (XMG1.2), and PE-conjugated anti-TNF-α (MP6-XT22), anti-IL-2 (JES6-5H4), or anti-granzyme B (clone 100) as described (52). The percentage of IFN-γ-positive cells was calculated by subtracting the background observed with the no peptide control.

For the degranulation assay, cells were incubated with 1 or 0.01 μg/ml of the appropriate peptide plus 10 U/ml IL-2, 10 μg/ml brefeldin A, 1×monensin (BioLegend), and 2.5 μg/ml FITC-conjugated anti-CD107a (1D4B) or control Ab in complete medium at 37°C for 5 h. Cells were stained with anti-CD8 Ab, then were fixed and rendered permeable before

Author Manuscript Author Manuscript Author Manuscript Author Manuscript

staining with allophycocyanin-conjugated anti-IFN-γ. Analysis was performed on a FACSCalibur flow cytometer using CellQuest software (BD Immunocytometry Systems).

Adoptive transfer and challenge experiments

For challenge experiments, MHV-68 infected B6 or 4-1BBL$^{-/-}$ mice were challenged at 4 mo postinfection with 10^6 PFU of rVV-ORF61 or ORF6 i.p., and expansion of virus-specific CD8$^+$ T cells in the spleen was enumerated by MHC/peptide tetramer staining at 5 days postchallenge.

For adoptive transfer experiments, spleens from MHV-68-infected B6 or 4-1BBL$^{-/-}$ mice were harvested at 2–4 mo postinfection, pooled, and 2×10^7 cells were injected into congenic B6 (B6-Ly5.2-Cr) mice i.v. (or vice versa, from congenic B6 mice to B6 or 4-1BBL$^{-/-}$ mice). Some cells from each group were kept for tetramer staining. One day after transfer, mice were challenged with 2.5×10^6 PFU of rVV-ORF6 i.p. Spleens were harvested 5 days postchallenge, and stained with the ORF6$_{487–495}$/D^b tetramer, anti-CD8, and anti-CD45.2 or anti-CD45.1 (which marks the donor population) Abs.

Virus neutralization assay

Serum was collected from mice infected with MHV-68. Six 3-fold dilutions of serum were made in duplicate, starting at a 1/50 dilution. The diluted serum samples were mixed with 40–50 PFU of MHV-68, and incubated on ice for 1 h. A total of 400 μl of the mixture was then added to NIH3T3 monolayers and were incubated at 37°C for 1 h. Two milliliters of medium containing CMC was added and the plates were cultured for 6 days at 37°C. Then, monolayers were fixed with methanol for 15 min, stained with Giemsa stain for at least 4 h, and plaques were counted microscopically. The fold dilution of serum which resulted in a 50% reduction in the number of plaques, compared with the no serum control, was calculated.

CD4$^+$ IFN-γ ELISPOT assay

The IFN-γ ELISPOT assays to quantify CD4$^+$ T cell responses were done as previously described (53). Briefly, CD4$^+$ cells were purified from MHV-68-infected spleens using a CD4$^+$ enrichment kit (StemCell Technologies). Purity was ~88–95%. A total of 10^5 purified cells were added to the first well in triplicate and were diluted at 3-fold dilutions for 4 wells. APCs were prepared by infecting naive splenocytes with 1 PFU/cell at 37°C for 1 h and subsequently irradiating the cells. A total of 5×10^5 APCs was added in each well. Cells were incubated at 37°C for 40–48 h and were developed and analyzed as previously described (52). The frequency of responding cells was corrected to normalize for the purity of CD4$^+$ T cells.

Statistical analysis

Values of p were calculated using the Student t test unless stated otherwise; $p < 0.05$ was considered significant.

Author Manuscript Author Manuscript Author Manuscript Author Manuscript

Results

Expression of 4-1BB by MHV-68-specific effector CD8+ T cells

Mice deficient in the 4-1BBL/4-1BB pathway exhibit defects mainly in the $CD8^+$ T cell response during viral infections (22–26, 30, 31, 54). Therefore, our initial studies on this pathway focused on the $CD8^+$ T cell response. To investigate the role of the 4-1BBL/4-1BB pathway in latent gammaherpesvirus infections, we first analyzed the expression of 4-1BB on virus-specific $CD8^+$ T cells during MHV-68 infection. 4-1BB expression on $CD8^+$ T cells in vivo has been observed during the early stages of activation, coinciding with expression of CD69 (55). The kinetics of 4-1BB expression during infection with HSV is also transient, although the peak of expression differs with the route of infection (27, 29). We sought to analyze the expression of 4-1BB on virus-specific $CD8^+$ T cells during MHV-68 infection, using MHC/peptide tetramer staining. As shown in Fig. 1, 4-1BB expression was detected on virus-specific $CD8^+$ T cells at day 10 postinfection for both the $ORF61_{524–531}/K^b$ and $ORF6_{487–495}/D^b$ epitopes. Similar to other models, expression in the spleen was very transient. At day 14, the peak of the $CD8^+$ T cell response, 4-1BB expression levels had gone down to minimal levels, and was not detectable during latency (day 85). In the mediastinal lymph node (MLN), 4-1BB expression was still detectable at day 14 though lower than that of day 10, but was not detectable at later time points (data not shown). Therefore, even during a latent infection where viral Ag is present in the microenvironment, 4-1BB expression on virus-specific $CD8^+$ T cells was restricted to the effector stage. The kinetics of 4-1BB expression on virus-specific $CD8^+$ T cells in the lung was similar to the spleen (data not shown).

Increased latent viral burden of MHV-68 in the absence of 4-1BBL

During influenza infection in mice, the 4-1BBL-4-1BB costimulatory pathway is required for long-term maintenance of memory $CD8^+$ T cells and secondary responses to viral challenge (22). However, the decay in memory $CD8^+$ T cell numbers occurred after the virus is cleared, hence does not affect the kinetics of viral control. Therefore, we first investigated whether the absence of the costimulatory pathway results in the loss of immune surveillance of the virus during the acute and latent stages of MHV-68 infection.

Control B6 mice and $4\text{-}1BBL^{-/-}$ mice were infected i.n. with 400 PFU of MHV-68 and the kinetics of viral replication and latency was observed. Viral replication in the lungs during the acute stage of infection in $4\text{-}1BBL^{-/-}$ mice was comparable to the control mice and no sign of viral recrudescence was observed in the lungs or the spleens (Fig. 2*A*). Even when the lungs and spleens were analyzed by a more sensitive in vitro-amplified plaque assay (see *Materials and Methods*), no signs of viral replication were detected (data not shown). MHV-68 infection causes splenomegaly at 2–3 wk postinfection and this was not affected by the absence of 4-1BBL (Fig. 2*B*).

Infection with MHV-68 results in a low level of persistence of the virus which can be detected by a sensitive quantitative PCR assay. At day 14 when the viral latent load in the spleen reaches its peak, the viral load did not differ between the two groups (Fig. 2*C*). However, during long-term latency, $4\text{-}1BBL^{-/-}$ mice exhibited significantly higher latent

Author Manuscript Author Manuscript Author Manuscript Author Manuscript

viral loads (~9 to 40-fold) compared with the B6 controls (Fig. 2*D*). The increase in viral load was also observed in the lungs (~5- to 18-fold) (Fig. 2*E*). These results indicate that there is a systemic defect in immune surveillance of latent MHV-68 infection in the absence of 4-1BBL.

Impaired virus-specific CD8$^+$ T cell function in the absence of 4-1BBL

The increase in latent viral load in the 4-1BBL$^{-/-}$ mice indicated a defect in immune surveillance of the virus. We hypothesized that similar to influenza infection, the memory CD8$^+$ T cell population was decreased in the absence of 4-1BBL, allowing the viral load to increase. Therefore, we measured the magnitude of the virus-specific CD8$^+$ T cell response by MHC/peptide tetramer staining. The initial expansion of ORF61$_{524–531}$/K^b and ORF6$_{487–495}$/D^b-specific CD8$^+$ T cells in the spleen, peripheral blood, and MLN was comparable to B6 controls (Fig. 3, *A*–*C*). Furthermore, in contrast to the influenza model and contrary to our predictions, the virus-specific CD8$^+$ T cell populations were maintained in the absence of 4-1BBL (Fig. 3*D*). Thus, the maintenance of memory CD8$^+$ T cells generated during latent MHV-68 infection was independent of 4-1BBL and did not account for the loss of immune surveillance in the 4-1BBL$^{-/-}$ mice.

Although the numbers of virus-specific memory CD8$^+$ T cells in 4-1BBL$^{-/-}$ mice were similar, the phenotype and function of these cells might be affected by the absence of 4-1BBL. Therefore, we first analyzed expression of activation/differentiation markers on virus-specific CD8$^+$ T cells during latency. We observed no significant differences in the expression of CD62L, CD27, CD127, CD122, CD25, and CD69 in 4-1BBL$^{-/-}$ mice (Fig. 4*A*). We also analyzed virus-specific memory CD8$^+$ T cells for IFN-γ and TNF-α production by intracellular cytokine staining upon restimulation with peptide in vitro. During both the effector (day 14) and memory (day 85) phase, no defects in cytokine production were observed in the 4-1BBL$^{-/-}$ mice when compared with control B6 mice (Fig. 4, *B* and *C*), even at a lower concentration of peptide (0.01 μg/ml, data not shown). Consistent with previous data, minimal IL-2 production was observed in both groups during latency (data not shown). These results show that the phenotype- and cytokine-producing ability of virus-specific CD8$^+$ T cells was not affected by the absence of 4-1BBL.

We next investigated whether the cytolytic function of MHV-68-specific CD8$^+$ T cells is maintained in the absence of 4-1BBL. In addition to cytokine production, killing of virus-infected targets is a major function of CD8$^+$ T cells. An in vivo CTL assay using ORF61$_{524–531}$- and ORF6$_{487–495}$-pulsed targets revealed that cytotoxicity against the ORF6$_{487–495}$/D^b epitope was impaired during latency (Fig. 5). To assess the mechanism of the defect in cytotoxicity, we analyzed the ability of ORF61$_{524–531}$/K^b- and ORF6$_{487–495}$/D^b-specific CD8$^+$ T cells to degranulate and produce granzyme B upon restimulation with viral peptides in vitro. We found that MHV-68-specific memory CD8$^+$ T cells in the 4-1BBL$^{-/-}$ mice were defective in their ability to degranulate upon restimulation (Fig. 6*A*). Intracellular levels of granzyme B upon stimulation with peptide were increased in the 4-1BBL$^{-/-}$ mice, which implies that the memory CD8$^+$ T cells were impaired in their ability to secrete granzyme B by degranulation (Fig. 6*B*). Similar results for both degranulation and granzyme B secretion were observed when cells were restimulated with a

Author Manuscript Author Manuscript Author Manuscript Author Manuscript

100-fold lower concentration of peptide (0.01 μg/ml, data not shown). These results indicate that in the 4-1BBL$^{-/-}$ mice, virus-specific CD8^{+} T cells are defective in their cytotoxicity, which is due to impairment in their ability to release their lytic granules.

Another important characteristic of memory CD8^{+} T cells is their ability to expand quickly in response to secondary Ag encounter. We challenged infected B6 or 4-1BBL$^{-/-}$ mice with rVV-ORF61 or rVV-ORF6 at 100^{+} days postinfection, and analyzed the expansion of virus-specific CD8^{+} T cells at 5 days postchallenge by MHC/peptide tetramer staining (Fig. 7*A*). CD8^{+} T cells specific for both epitopes were able to mount a robust secondary response to the rVVs, in contrast to the primary response observed in naive B6 mice. However, in the absence of 4-1BBL, the virus-specific memory CD8^{+} T cells were impaired in mounting a secondary response (Fig. 7*A*).

The defective secondary expansion observed in the 4-1BBL$^{-/-}$ mice could be due to two reasons: either 4-1BBL/4-1BB costimulation is required to prime and maintain the virus-specific CD8^{+} T cells properly for them to differentiate into functionally competent memory cells or 4-1BBL/4-1BB costimulation is simply required during secondary exposure to Ag. To investigate the two possibilities, we first analyzed whether 4-1BB is re-expressed on virus-specific CD8^{+} T cells upon secondary expansion. As shown in Fig. 7*B*, 4-1BB was rapidly up-regulated on ORF6-specific CD8^{+} T cells upon challenge with rVV-ORF6. The up-regulation was very transient and the kinetics were significantly more rapid than the CD8^{+} T cell response specific for the vaccinia virus immunodominant B8R$_{20–27}$/K^{b} epitope (56), which represents a primary response. Because 4-1BB is expressed both during priming and the secondary response, 4-1BB costimulation could be required at either stage of the response or at both.

To investigate at which stage 4-1BB costimulation is required to mount an efficient secondary response, we performed a series of adoptive transfer experiments. First, to explore whether the impaired secondary expansion in the 4-1BBL$^{-/-}$ mice was due to defective priming of the virus-specific CD8^{+} T cells, we designed an adoptive transfer experiment shown in Fig. 7*C*. Splenocytes (2×10^{7}) from MHV-68 infected B6 or 4-1BBL$^{-/-}$ mice at 2–4 mo postinfection were adoptively transferred into naive congenic (CD45.1^{+}) B6 mice and the mice were challenged 1 day later with rVV-ORF6 and secondary expansion was monitored at day 5 postchallenge. Therefore, virus-specific CD8^{+} T cells differentiated in the absence of 4-1BBL, but the pathway was present during secondary expansion. Upon rVV-ORF6 challenge, secondary expansion was significantly reduced when the ORF6-specific memory CD8^{+} T cells were derived from 4-1BBL$^{-/-}$ donors (Fig. 7*C*). The experiment suggests that 4-1BB costimulation is required during priming to mount a robust secondary response. In the second set of adoptive transfer experiments, we investigated whether 4-1BB costimulation is required during the secondary response. Splenocytes from MHV-68-infected B6 (CD45.1) mice were transferred into B6 (CD45.2) or 4-1BBL$^{-/-}$ mice, challenged 1 day later with rVV-ORF6, and secondary expansion was observed 5 days postchallenge. Secondary expansion was significantly reduced when this pathway was absent, suggesting that it is also required during the secondary response (Fig. 7*D*), which is consistent with its expression profile (Fig. 7*B*). These results together suggest that a robust

Author Manuscript Author Manuscript Author Manuscript Author Manuscript

secondary response requires 4-1BBL/4-1BB costimulation both during priming and the recall response.

CD4$^+$ T cell and humoral responses to MHV-68 infection in 4-1BBL$^{-/-}$ mice

Due to the defects observed in the antiviral CD8$^+$ T cell response, we were interested in whether the absence of 4-1BBL results in defects in the CD4$^+$ T cell and humoral response against MHV-68 infection. The primary virus-specific CD4$^+$ T cell response at day 20 postinfection was significantly reduced in 4-1BBL$^{-/-}$ mice (Fig. 8*A*), but the frequencies during latency were comparable to the B6 controls (Fig. 8*B*). As for the humoral response, virus-neutralizing Abs were detected in the serum of MHV-68 infected 4-1BBL$^{-/-}$ mice at 20 and 138 days postinfection (Fig. 8, *C* and *D*). The frequency of memory-phenotype (CD19$^+$IgD^{low} CD38^{high}) B cells, the major reservoirs for the virus, was also comparable to B6 controls (data not shown). Therefore, although 4-1BBL is required for an efficient primary virus-specific CD4$^+$ T cell response, it appears to play no major role in memory CD4$^+$ T cell responses and induction of the humoral response against MHV-68 infection.

Discussion

The role of costimulation in chronic viral infections is an understudied topic, despite the wealth of knowledge on the effects of costimulatory signals in antitumor immune responses, transplantation, autoimmunity, and antiviral immunity in acute infections. Several lines of evidence support the importance of certain costimulatory molecules in the control of chronic infections. The CD40L/CD40 pathway, which is critical for humoral immune responses and in many cellular responses, has been shown to be crucial for the control of several LCMV strains (57, 58) and MHV-68 (44, 46). CD80/CD86 and its ligands are required for the efficient control of LCMV clone 13 (59) and MHV-68 (47). Furthermore, in addition to the CD40 and CD80/CD86 pathways, CD70/CD27 costimulation has been shown to affect virus-CD8$^+$ T cell responses during persistent mouse polyoma virus infection (60) or the consequences of chronic LCMV infection (61). Studies have shown that different costimulatory signals affect various aspects and function of the immune system (2, 4); thus, how these costimulatory molecules are involved in the surveillance of chronic infections is a subject of interest.

The impact of the 4-1BBL/4-1BB costimulatory pathway in antiviral immunity has been studied in several viral infection models using gene knockout mice. Induction of Ab responses to LCMV, influenza virus, and vesicular stomatitis virus (VSV) is not affected in 4-1BBL$^{-/-}$ or 4-1BB$^{-/-}$ mice, indicating that 4-1BBL costimulation is not required for humoral immunity to viral infections (22, 28, 30). Similarly, this pathway does not significantly affect antiviral CD4$^+$ T cell responses to LCMV and influenza virus infection (22, 30), although costimulation of Ag-specific CD4$^+$ T cell responses by 4-1BB has been reported (62) and our data suggest that primary CD4$^+$ T cell responses to MHV-68 are affected. In contrast, increased proliferation of 4-1BB$^{-/-}$ OVA-specific CD4$^+$ T cells has also been observed (63), but evidence that this pathway can transmit negative signals has not been observed in virus infection models. 4-1BBL costimulation seems to have a stronger influence on the antiviral CD8$^+$ T cell response, as reduced responses are observed during

Author Manuscript Author Manuscript Author Manuscript Author Manuscript

LCMV infection (30), i.n. infection with influenza (26), and VSV infection (28). Interestingly, loss of virus-specific memory $CD8^+$ T cells is observed after influenza infection (22). Furthermore, protective immunity against LCMV challenge after peptide vaccination is defective in the absence of 4-1BBL (31), pointing to an important role of this pathway in long-term $CD8^+$ T cell responses. Therefore, we suspected that the 4-1BBL/4-1BB costimulatory pathway might be playing a significant role in the control of chronic viral infection.

Infection with MHV-68 results in a latent infection where viral Ag persists for the lifetime of the animal. Therefore, virus-specific $CD8^+$ T cells periodically encounter Ag as the virus persists throughout the lifetime of the animal. Even so, 4-1BB expression on virus-specific $CD8^+$ T cells was restricted to the effector stage (Fig. 1). Therefore, the effects of this pathway on the virus-specific $CD8^+$ T cell response is most likely restricted to this stage, although a low level of 4-1BB expression below the level of detection by flow cytometry cannot be ruled out.

When the kinetics of viral latency and replication were examined, we observed a significant increase in the latent viral load in both the spleen and the lung during long-term latency (Fig. 2, *D* and *E*). These results indicated a defect in immune surveillance of MHV-68 in 4-1BBL$^{-/-}$ mice. Interestingly, acute infection was not affected (Fig. 2, *A* and *C*), and despite the increase in latent viral load, no evidence of viral reactivation was observed in both the lung and the spleen (Fig. 2*A*). This phenotype is particularly interesting, because it differs considerably from other genetically deficient mice that are unable to control MHV-68 infection. In MHC class II$^{-/-}$, CD40L$^{-/-}$, or CD40$^{-/-}$ mice, the virus reactivates to high titers in the lungs and the latent viral load in the spleen are also increased (44–46) (S. Fuse and E. J. Usherwood, unpublished observations). In CD80/CD86$^{-/-}$ mice, the degree of virus reactivation in the lungs is lower and the latent viral load in the spleen is comparable to wild-type mice (47). We believe that the key difference between these strains and the 4-1BBL$^{-/-}$ mice is the antiviral Ab response, which can immediately neutralize any virus that reactivates. 4-1BBL$^{-/-}$ mice are fully capable of inducing neutralizing Abs against MHV-68 (Fig. 8, *C* and *D*), where as the strains mentioned above are severely impaired in their humoral response (44–47). The antiviral $CD4^+$ T cell response is affected during the primary response in the 4-1BBL$^{-/-}$ mice (Fig. 8*A*), but not during latency (Fig. 8*B*), and therefore is unlikely to be responsible for the increased viral load during chronic infection. The only arm of the immune response that was found to be defective during latency in the absence of 4-1BBL was the $CD8^+$ T cell response (Figs. 5–7), and we propose that the functional defects observed in the antiviral $CD8^+$ T cell response causes the increase in latent viral load. An increase in the latent viral load in the absence of $CD8^+$ T cells has been documented previously (37, 42). There is a possibility that very low levels of viral reactivation may be occurring but is neutralized by the presence of Abs and virus-specific $CD4^+$ T cells; however, we were not able to detect any evidence of viral reactivation in these mice during long-term latency.

Aside from the cellular response, the 4-1BBL/4-1BB pathway has been shown to affect BMMCs (5), NK/NKT cells (64), as well as neutrophils during *Listeria monocytogenes* infection (65). However, treatment with anti-NK1.1 does not have any impact on MHV-68

Author Manuscript Author Manuscript Author Manuscript Author Manuscript

infection (66), which suggests that the phenotype observed in the 4-1BBL$^{-/-}$ mice is not due to defects in NK/NKT cells. The roles of MCs or neutrophils in the control of MHV-68 infection are currently unknown and we cannot rule out the possibility that the loss of immune surveillance in the 4-1BBL$^{-/-}$ mice could partially be due to a defects in these subsets.

Because 4-1BBL costimulation has been reported to affect mainly the antiviral CD8^{+} T cell response, we analyzed the CD8^{+} T cell response to MHV-68 in detail. Unlike the observations made in LCMV, influenza, or VSV models (26, 28, 30), the primary response to MHV-68 in 4-1BBL$^{-/-}$ mice was comparable to wild-type B6 mice (Fig. 3, *A–C*,). Furthermore, the number of virus-specific memory CD8^{+} T cells was maintained in the absence of 4-1BBL (Fig. 3*D*). However, despite the similarities in the magnitude of the response, certain functions of the memory CD8^{+} T cells were impaired. First, cytotoxicity to target cells pulsed with ORF6 peptide in vivo was significantly reduced (Fig. 5). Accordingly, virus-specific CD8^{+} T cells were impaired in their ability to degranulate upon restimulation with peptide in vitro (Fig. 6*A*). Secretion of granzyme B by degranulation upon restimulation was also impaired in 4-1BBL$^{-/-}$ mice (Fig. 6*B*).

In addition to cytotoxicity, the ability of memory CD8^{+} T cells to mount a recall response to secondary Ag encounter was impaired (Fig. 7*A*). Secondary responses to influenza infection and to LCMV challenge after peptide vaccination have been previously reported (22, 31). In the influenza model, 4-1BBL was required both during maintenance of memory CD8^{+} T cells and during secondary expansion (23). We observed a rapid re-expression of 4-1BB on virus-specific CD8^{+} T cells during the recall response to rVV-ORF6 (Fig. 7*B*). Results from adoptive transfer experiments suggested that this pathway is required both during priming and the secondary response for a robust recall response (Fig. 7, *C* and *D*), matching their expression pattern. Our adoptive transfer experiments did not discriminate whether the initial 4-1BB signal is required during priming or maintenance of virus-specific CD8^{+} T cells. However, because 4-1BB expression is restricted to the effector phase (Fig. 1), it is likely that 4-1BBL/4-1BB costimulation during the priming phase programs the MHV-68-specific CD8^{+} T cells into functionally competent memory cells capable of mounting a robust recall response.

Despite the defects in cytotoxicity and recall response observed in the 4-1BBL$^{-/-}$ mice, the phenotype of the virus-specific memory CD8^{+} T cells and cytokine (IFN-γ and TNF-α) production by the memory cells was unaltered in 4-1BBL$^{-/-}$ mice. In the absence of the CD80/CD86-CD28 costimulatory pathway, defects in IFN-γ production and recall response as well as alterations in phenotype were observed, but cytotoxicity was not affected (47). The two studies together elucidate an interesting point where different functions of MHV-68-specific memory CD8^{+} T cells are controlled by different costimulatory pathways.

In summary, we report the role of 4-1BBL/4-1BB costimulation in the immune surveillance of MHV-68 infection. 4-1BBL$^{-/-}$ mice were capable of controlling the acute infection and no signs of viral reactivation were observed. However, significantly increased levels of latent viral load were detected in the lungs and spleens during long-term latency. The absence of 4-1BBL did not affect the induction of virus neutralizing Abs, or the virus-

Author Manuscript Author Manuscript Author Manuscript Author Manuscript

specific memory $CD4^+$ T cell response. The magnitude of the $CD8^+$ T cell response was comparable to wild-type mice during the effector and memory phase, but certain functions, such as cytotoxicity and their ability to mount a secondary response, were severely impaired in the absence of this pathway. Our study on the role of 4-1BBL/4-1BB costimulation in murine gammaherpesvirus immune surveillance adds important information to our short list of knowledge on the role of costimulatory molecules in chronic infections. Furthermore, increasing information on this list should benefit immunotherapeutic interventions of chronic infections such as therapeutic vaccination.

Acknowledgments

We express our gratitude to Dr. William Green and Amgen for mice and permission to use them for our studies. We also thank Dr. Alice Givan and Gary Ward for assistance in flow cytometry, and Dr. Joshua Obar and Weijun Zhang for fruitful discussions.

References

1. Bertram EM, Dawicki W, Watts TH. Role of T cell costimulation in anti-viral immunity. Semin Immunol. 2004; 16:185–196. [PubMed: 15130503]
2. Greenwald RJ, Freeman GJ, Sharpe AH. The B7 family revisited. Annu Rev Immunol. 2005; 23:515–548. [PubMed: 15771580]
3. Whitmire JK, Ahmed R. Costimulation in antiviral immunity: differential requirements for $CD4^+$ and $CD8^+$ T cell responses. Curr Opin Immunol. 2000; 12:448–455. [PubMed: 10899032]
4. Watts TH. TNF/TNFR family members in costimulation of T cell responses. Annu Rev Immunol. 2005; 23:23–68. [PubMed: 15771565]
5. Nishimoto H, Lee SW, Hong H, Potter KG, Maeda-Yamamoto M, Kinoshita T, Kawakami Y, Mittler RS, Kwon BS, Ware CF, et al. Costimulation of mast cells by 4-1BB, a member of the tumor necrosis factor receptor superfamily, with the high-affinity IgE receptor. Blood. 2005; 106:4241–4248. [PubMed: 16123219]
6. Takahashi C, Mittler RS, Vella AT. Cutting edge: 4-1BB is a bona fide CD8 T cell survival signal. J Immunol. 1999; 162:5037–5040. [PubMed: 10227968]
7. Shuford WW, Klussman K, Tritchler DD, Loo DT, Chalupny J, Siadak AW, Brown TJ, Emswiler J, Raecho H, Larsen CP, et al. 4-1BB costimulatory signals preferentially induce $CD8^+$ T cell proliferation and lead to the amplification in vivo of cytotoxic T cell responses. J Exp Med. 1997; 186:47–55. [PubMed: 9206996]
8. Croft M. Co-stimulatory members of the TNFR family: keys to effective T-cell immunity? Nat Rev Immunol. 2003; 3:609–620. [PubMed: 12974476]
9. Ye Z, Hellstrom I, Hayden-Ledbetter M, Dahlin A, Ledbetter JA, Hellstrom KE. Gene therapy for cancer using single-chain Fv fragments specific for 4-1BB. Nat Med. 2002; 8:343–348. [PubMed: 11927939]
10. Melero I, Shuford WW, Newby SA, Aruffo A, Ledbetter JA, Hellstrom KE, Mittler RS, Chen L. Monoclonal antibodies against the 4-1BB T-cell activation molecule eradicate established tumors. Nat Med. 1997; 3:682–685. [PubMed: 9176498]
11. Kim JA, Averbook BJ, Chambers K, Rothchild K, Kjaergaard J, Papay R, Shu S. Divergent effects of 4-1BB antibodies on antitumor immunity and on tumor-reactive T-cell generation. Cancer Res. 2001; 61:2031–2037. [PubMed: 11280763]
12. Ito F, Li Q, Shreiner AB, Okuyama R, Jure-Kunkel MN, Teitz-Tennenbaum S, Chang AE. Anti-CD137 monoclonal antibody administration augments the antitumor efficacy of dendritic cell-based vaccines. Cancer Res. 2004; 64:8411–8419. [PubMed: 15548712]
13. Blazar BR, Kwon BS, Panoskaltsis-Mortari A, Kwak KB, Peschon JJ, Taylor PA. Ligation of 4-1BB (CDw137) regulates graft-versus-host disease, graft-versus-leukemia, and graft rejection in allogeneic bone marrow transplant recipients. J Immunol. 2001; 166:3174–3183. [PubMed: 11207270]

Author Manuscript Author Manuscript Author Manuscript Author Manuscript

14. Fukushima A, Yamaguchi T, Ishida W, Fukata K, Mittler RS, Yagita H, Ueno H. Engagement of 4-1BB inhibits the development of experimental allergic conjunctivitis in mice. J Immunol. 2005; 175:4897–4903. [PubMed: 16210591]
15. Kwon B, Lee HW, Kwon BS. New insights into the role of 4-1BB in immune responses: beyond $CD8^+$ T cells. Trends Immunol. 2002; 23:378–380. [PubMed: 12133793]
16. Mittler RS, Bailey TS, Klussman K, Trailsmith MD, Hoffmann MK. Anti-4-1BB monoclonal antibodies abrogate T cell-dependent humoral immune responses in vivo through the induction of helper T cell anergy. J Exp Med. 1999; 190:1535–1540. [PubMed: 10562327]
17. Myers L, Takahashi C, Mittler RS, Rossi RJ, Vella AT. Effector CD8 T cells possess suppressor function after 4-1BB and Toll-like receptor triggering. Proc Natl Acad Sci USA. 2003; 100:5348–5353. [PubMed: 12695569]
18. Polte T, Foell J, Werner C, Hoymann HG, Braun A, Burdach S, Mittler RS, Hansen G. CD137-mediated immunotherapy for allergic asthma. J Clin Invest. 2006; 116:1025–1036. [PubMed: 16528411]
19. Seo SK, Choi JH, Kim YH, Kang WJ, Park HY, Suh JH, Choi BK, Vinay DS, Kwon BS. 4-1BB-mediated immunotherapy of rheumatoid arthritis. Nat Med. 2004; 10:1088–1094. [PubMed: 15448685]
20. Sun Y, Lin X, Chen HM, Wu Q, Subudhi SK, Chen L, Fu YX. Administration of agonistic anti-4-1BB monoclonal antibody leads to the amelioration of experimental autoimmune encephalomyelitis. J Immunol. 2002; 168:1457–1465. [PubMed: 11801689]
21. Zheng G, Wang B, Chen A. The 4-1BB costimulation augments the proliferation of $CD4^+CD25^+$ regulatory T cells. J Immunol. 2004; 173:2428–2434. [PubMed: 15294956]
22. Bertram EM, Lau P, Watts TH. Temporal segregation of 4-1BB versus CD28-mediated costimulation: 4-1BB ligand influences T cell numbers late in the primary response and regulates the size of the T cell memory response following influenza infection. J Immunol. 2002; 168:3777–3785. [PubMed: 11937529]
23. Bertram EM, Dawicki W, Sedgmen B, Bramson JL, Lynch DH, Watts TH. A switch in costimulation from CD28 to 4-1BB during primary versus secondary CD8 T cell response to influenza in vivo. J Immunol. 2004; 172:981–988. [PubMed: 14707071]
24. DeBenedette MA, Wen T, Bachmann MF, Ohashi PS, Barber BH, Stocking KL, Peschon JJ, Watts TH. Analysis of 4-1BB ligand (4-1BBL)-deficient mice and of mice lacking both 4-1BBL and CD28 reveals a role for 4-1BBL in skin allograft rejection and in the cytotoxic T cell response to influenza virus. J Immunol. 1999; 163:4833–4841. [PubMed: 10528184]
25. Halstead ES, Mueller YM, Altman JD, Katsikis PD. In vivo stimulation of CD137 broadens primary antiviral $CD8^+$ T cell responses. Nat Immunol. 2002; 3:536–541. [PubMed: 12021777]
26. Hendriks J, Xiao Y, Rossen JW, van der Sluijs KF, Sugamura K, Ishii N, Borst J. During viral infection of the respiratory tract, CD27, 4-1BB, and OX40 collectively determine formation of $CD8^+$ memory T cells and their capacity for secondary expansion. J Immunol. 2005; 175:1665–1676. [PubMed: 16034107]
27. Kim YH, Seo SK, Choi BK, Kang WJ, Kim CH, Lee SK, Kwon BS. 4-1BB costimulation enhances HSV-1-specific $CD8^+$ T cell responses by the induction of $CD11c^+CD8^+$ T cells. Cell Immunol. 2005; 238:76–86. [PubMed: 16524567]
28. Kwon BS, Hurtado JC, Lee ZH, Kwack KB, Seo SK, Choi BK, Koller BH, Wolisi G, Broxmeyer HE, Vinay DS. Immune responses in 4-1BB (CD137)-deficient mice. J Immunol. 2002; 168:5483–5490. [PubMed: 12023342]
29. Seo SK, Park HY, Choi JH, Kim WY, Kim YH, Jung HW, Kwon B, Lee HW, Kwon BS. Blocking 4-1BB/4-1BB ligand interactions prevents herpetic stromal keratitis. J Immunol. 2003; 171:576–583. [PubMed: 12847221]
30. Tan JT, Whitmire JK, Ahmed R, Pearson TC, Larsen CP. 4-1BB ligand, a member of the TNF family, is important for the generation of antiviral CD8 T cell responses. J Immunol. 1999; 163:4859–4868. [PubMed: 10528187]
31. Tan JT, Whitmire JK, Murali-Krishna K, Ahmed R, Altman JD, Mittler RS, Sette A, Pearson TC, Larsen CP. 4-1BB costimulation is required for protective anti-viral immunity after peptide vaccination. J Immunol. 2000; 164:2320–2325. [PubMed: 10679066]

Author Manuscript Author Manuscript Author Manuscript Author Manuscript

32. Antman K, Chang Y. Kaposi's sarcoma. N Engl J Med. 2000; 342:1027–1038. [PubMed: 10749966]
33. Drew WL. Cytomegalovirus infection in patients with AIDS. Clin Infect Dis. 1992; 14:608–615. [PubMed: 1313313]
34. Kimberlin DW, Rouse DJ. Clinical practice: genital herpes. N Engl J Med. 2004; 350:1970–1977. [PubMed: 15128897]
35. Young LS, Rickinson AB. Epstein-Barr virus: 40 years on. Nat Rev Cancer. 2004; 4:757–768. [PubMed: 15510157]
36. Ehtisham S, Sunil-Chandra NP, Nash AA. Pathogenesis of murine gammaherpesvirus infection in mice deficient in CD4 and CD8 T cells. J Virol. 1993; 67:5247–5252. [PubMed: 8394447]
37. Stevenson PG, Cardin RD, Christensen JP, Doherty PC. Immunological control of a murine gammaherpesvirus independent of $CD8^+$ T cells. J Gen Virol. 1999; 80:477–483. [PubMed: 10073710]
38. Flano E, Husain SM, Sample JT, Woodland DL, Blackman MA. Latent murine gamma-herpesvirus infection is established in activated B cells, dendritic cells, and macrophages. J Immunol. 2000; 165:1074–1081. [PubMed: 10878386]
39. Stewart JP, Usherwood EJ, Ross A, Dyson H, Nash T. Lung epithelial cells are a major site of murine gammaherpesvirus persistence. J Exp Med. 1998; 187:1941–1951. [PubMed: 9625754]
40. Sunil-Chandra NP, Efstathiou S, Nash AA. Murine gammaherpesvirus 68 establishes a latent infection in mouse B lymphocytes in vivo. J Gen Virol. 1992; 73:3275–3279. [PubMed: 1469366]
41. Weck KE, Kim SS, Virgin HI, Speck SH. Macrophages are the major reservoir of latent murine gammaherpesvirus 68 in peritoneal cells. J Virol. 1999; 73:3273–3283. [PubMed: 10074181]
42. Kim IJ, Flano E, Woodland DL, Blackman MA. Antibody-mediated control of persistent gamma-herpesvirus infection. J Immunol. 2002; 168:3958–3964. [PubMed: 11937552]
43. Tibbetts SA, van Dyk LF, Speck SH, Virgin HW IV. Immune control of the number and reactivation phenotype of cells latently infected with a gammaherpesvirus. J Virol. 2002; 76:7125–7132. [PubMed: 12072512]
44. Brooks JW, Hamilton-Easton AM, Christensen JP, Cardin RD, Hardy CL, Doherty PC. Requirement for CD40 ligand, $CD4^+$ T cells, and B cells in an infectious mononucleosis-like syndrome. J Virol. 1999; 73:9650–9654. [PubMed: 10516078]
45. Cardin RD, Brooks JW, Sarawar SR, Doherty PC. Progressive loss of $CD8^+$ T cell-mediated control of a gamma-herpesvirus in the absence of $CD4^+$ T cells. J Exp Med. 1996; 184:863–871. [PubMed: 9064346]
46. Lee BJ, Reiter SK, Anderson M, Sarawar SR. $CD28^{-/-}$ mice show defects in cellular and humoral immunity but are able to control infection with murine gammaherpesvirus 68. J Virol. 2002; 76:3049–3053. [PubMed: 11861872]
47. Fuse S, Obar JJ, Bellfy S, Leung EK, Zhang W, Usherwood EJ. CD80 and CD86 control antiviral $CD8^+$ T-cell function and immune surveillance of murine gammaherpesvirus 68. J Virol. 2006; 80:9159–9170. [PubMed: 16940527]
48. Lyon AB, Sarawar SR. Differential requirement for CD28 and CD80/86 pathways of costimulation in the long-term control of murine gammaherpesvirus-68. Virology. 2006; 356:50–56. [PubMed: 16934307]
49. Sunil-Chandra NP, Efstathiou S, Arno J, Nash AA. Virological and pathological features of mice infected with murine gamma-herpesvirus 68. J Gen Virol. 1992; 73:2347–2356. [PubMed: 1328491]
50. Stevenson PG, Belz GT, Castrucci MR, Altman JD, Doherty PC. A gamma-herpesvirus sneaks through a $CD8^+$ T cell response primed to a lytic-phase epitope. Proc Natl Acad Sci USA. 1999; 96:9281–9286. [PubMed: 10430934]
51. Usherwood EJ, Ward KA, Blackman MA, Stewart JP, Woodland DL. Latent antigen vaccination in a model gammaherpesvirus infection. J Virol. 2001; 75:8283–8288. [PubMed: 11483773]
52. Usherwood EJ. A new approach to epitope confirmation by sampling effector/memory T cells migrating to the lung. J Immunol Methods. 2002; 266:135–142. [PubMed: 12133630]
53. Christensen JP, Doherty PC. Quantitative analysis of the acute and long-term $CD4^+$ T-cell response to a persistent gammaherpesvirus. J Virol. 1999; 73:4279–4283. [PubMed: 10196325]

Author Manuscript Author Manuscript Author Manuscript Author Manuscript

54. Dawicki W, Bertram EM, Sharpe AH, Watts TH. 4-1BB and OX40 act independently to facilitate robust CD8 and CD4 recall responses. J Immunol. 2004; 173:5944–5951. [PubMed: 15528328]
55. Dawicki W, Watts TH. Expression and function of 4-1BB during CD4 versus CD8 T cell responses in vivo. Eur J Immunol. 2004; 34:743–751. [PubMed: 14991604]
56. Tscharke DC, Karupiah G, Zhou J, Palmore T, Irvine KR, Haeryfar SM, Williams S, Sidney J, Sette A, Bennink JR, Yewdell JW. Identification of poxvirus $CD8^+$ T cell determinants to enable rational design and characterization of smallpox vaccines. J Exp Med. 2005; 201:95–104. [PubMed: 15623576]
57. Thomsen AR, Nansen A, Christensen JP, Andreasen SO, Marker O. CD40 ligand is pivotal to efficient control of virus replication in mice infected with lymphocytic choriomeningitis virus. J Immunol. 1998; 161:4583–4590. [PubMed: 9794385]
58. Whitmire JK, Flavell RA, Grewal IS, Larsen CP, Pearson TC, Ahmed R. CD40-CD40 ligand costimulation is required for generating antiviral CD4 T cell responses but is dispensable for CD8 T cell responses. J Immunol. 1999; 163:3194–3201. [PubMed: 10477587]
59. Christensen JE, Christensen JP, Kristensen NN, Hansen NJ, Stryhn A, Thomsen AR. Role of CD28 co-stimulation in generation and maintenance of virus-specific T cells. Int Immunol. 2002; 14:701–711. [PubMed: 12096029]
60. Kemball CC, Lee ED, Szomolanyi-Tsuda E, Pearson TC, Larsen CP, Lukacher AE. Costimulation requirements for antiviral $CD8^+$ T cells differ for acute and persistent phases of polyoma virus infection. J Immunol. 2006; 176:1814–1824. [PubMed: 16424212]
61. Matter M, Odermatt B, Yagita H, Nuoffer JM, Ochsenbein AF. Elimination of chronic viral infection by blocking CD27 signaling. J Exp Med. 2006; 203:2145–2155. [PubMed: 16923852]
62. Gramaglia I, Cooper D, Miner KT, Kwon BS, Croft M. Co-stimulation of antigen-specific CD4 T cells by 4-1BB ligand. Eur J Immunol. 2000; 30:392–402. [PubMed: 10671194]
63. Lee SW, Vella AT, Kwon BS, Croft M. Enhanced CD4 T cell responsiveness in the absence of 4-1BB. J Immunol. 2005; 174:6803–6808. [PubMed: 15905521]
64. Vinay DS, Choi BK, Bae JS, Kim WY, Gebhardt BM, Kwon BS. CD137-deficient mice have reduced NK/NKT cell numbers and function, are resistant to lipopolysaccharide-induced shock syndromes, and have lower IL-4 responses. J Immunol. 2004; 173:4218–4229. [PubMed: 15356173]
65. Lee SC, Ju SA, Pack HN, Heo SK, Suh JH, Park SM, Choi BK, Kwon BS, Kim BS. 4-1BB (CD137) is required for rapid clearance of *Listeria monocytogenes* infection. Infect Immun. 2005; 73:5144–5151. [PubMed: 16041031]
66. Usherwood EJ, Meadows SK, Crist SG, Bellfy SC, Sentman CL. Control of murine gammaherpesvirus infection is independent of NK cells. Eur J Immunol. 2005; 35:2956–2961. [PubMed: 16134085]

Author Manuscript Author Manuscript Author Manuscript Author Manuscript

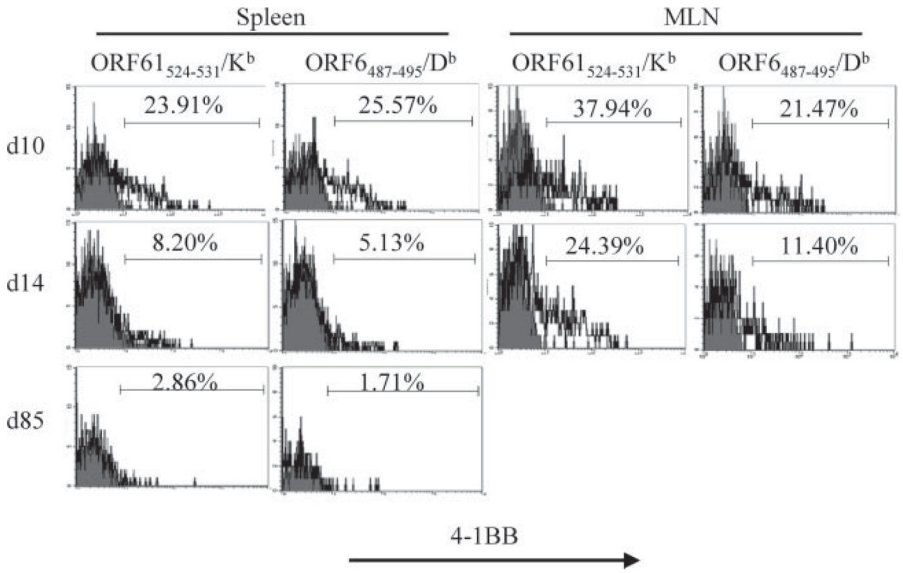

FIGURE 1.

4-1BB is expressed on virus-specific effector CD8$^+$ T cells. 4-1BB expression on CD8$^+$ T cells specific for the ORF61$_{524–531}$/K^b and ORF6$_{487–495}$/D^b epitopes was analyzed. Shaded histograms, isotype control; bold lines, anti-4-1BB. Representative plots from the spleen and MLN at indicated time points are shown. Cells are gated on CD8$^+$tetramer$^+$ cells.

Author Manuscript Author Manuscript Author Manuscript Author Manuscript

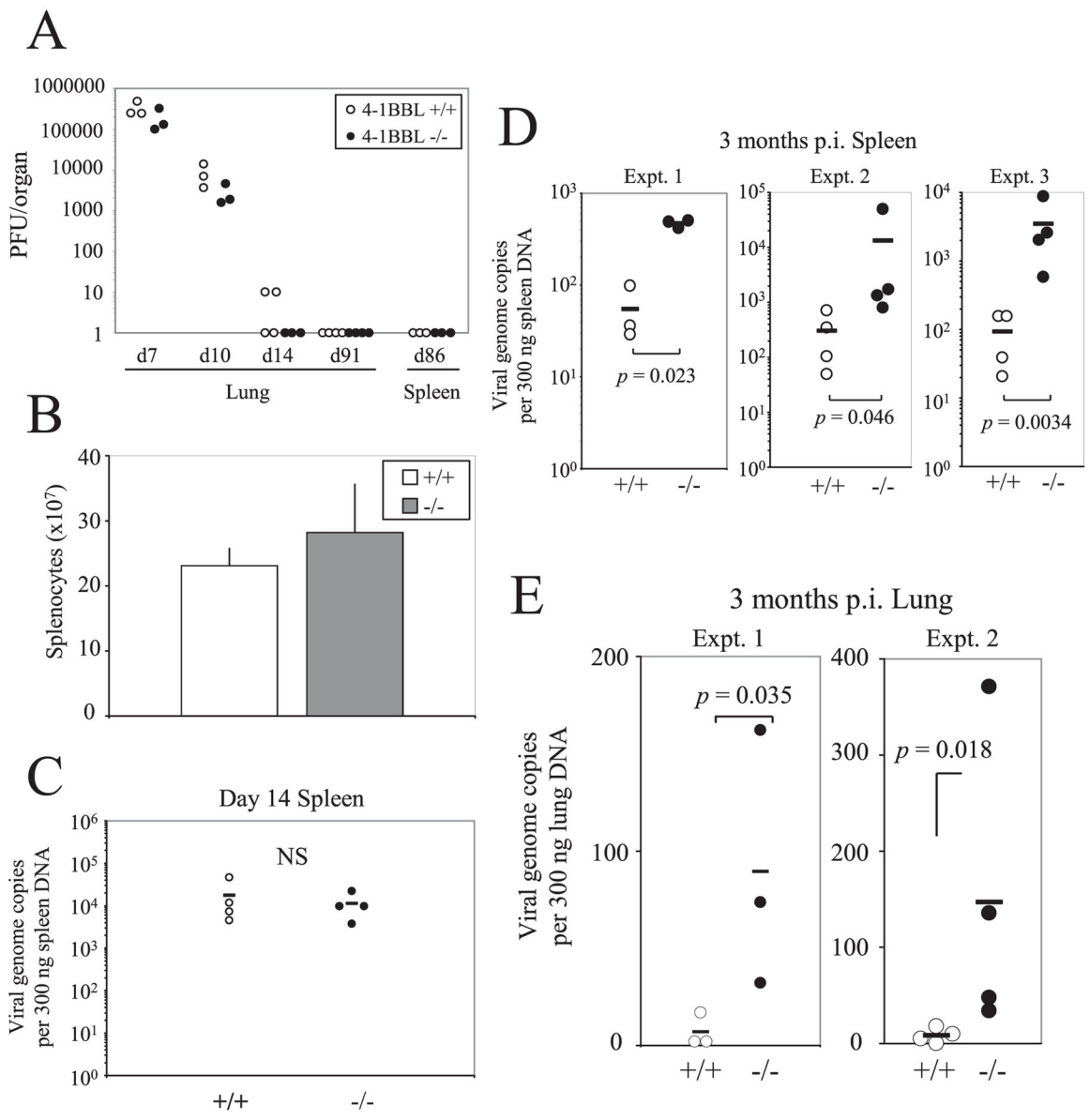

FIGURE 2.

Increased latent viral burden in the absence of 4-1BBL. *A*, Lungs and spleens were harvested at indicated time points postinfection and were assayed for viral titers by a standard plaque assay using NIH3T3 cells. Each point represents data from an individual animal. *B*, Total number of splenocytes at day 14 postinfection is graphed. Error bars indicate SD. *C–E*, The latent viral load was measured in the spleens at day 14 postinfection (*C*), at 3 mo postinfection (*D*), or in the lungs 3 mo postinfection (*E*) by QF-PCR for the *ORF50* gene. Each point represents data from an individual animal and horizontal bars indicate mean values. Representative data from two to three independent experiments (*A–C*) or individual experiments (*D* and *E*) are shown.

Author Manuscript Author Manuscript Author Manuscript Author Manuscript

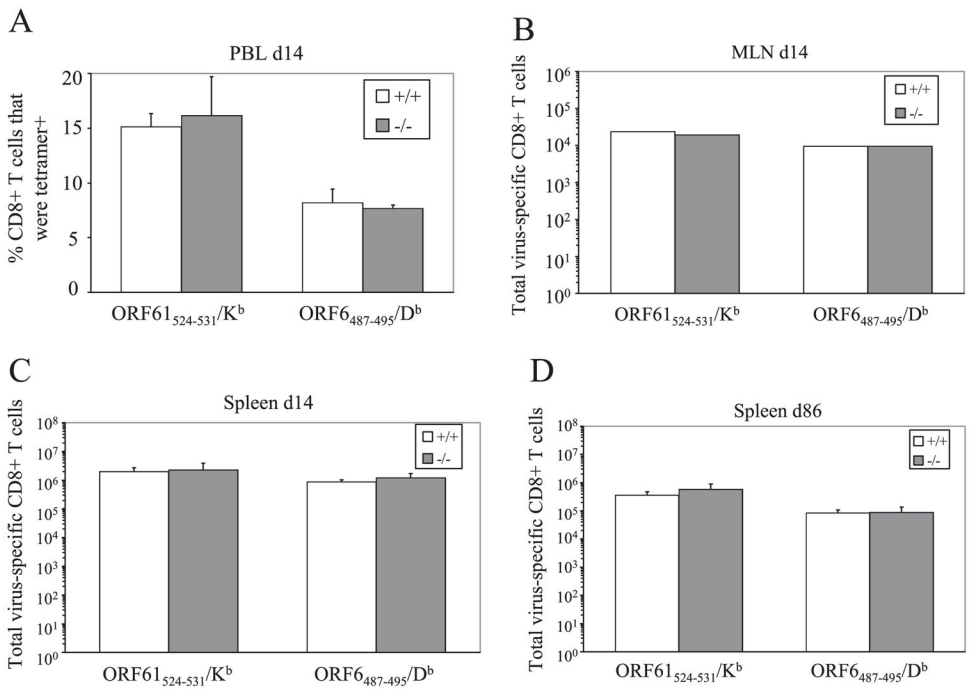

FIGURE 3.

The magnitude of the virus-specific $CD8^+$ T cell response is 4-1BBL independent. $CD8^+$ T cells specific for the $ORF61_{524–531}/K^b$ and $ORF6_{487–495}/D^b$ epitopes in the peripheral blood (*A*), MLN (*B*), and spleen (*C* and *D*) were quantified at indicated time points by MHC/tetramer staining. The percentage (*A*), or the total number (*B–D*), of $CD8^+$ T cells specific for each epitope are graphed (error bars indicate SD). MLN were pooled for each group. Representative data from two independent experiments with three to four mice per group are shown.

Author Manuscript Author Manuscript Author Manuscript Author Manuscript

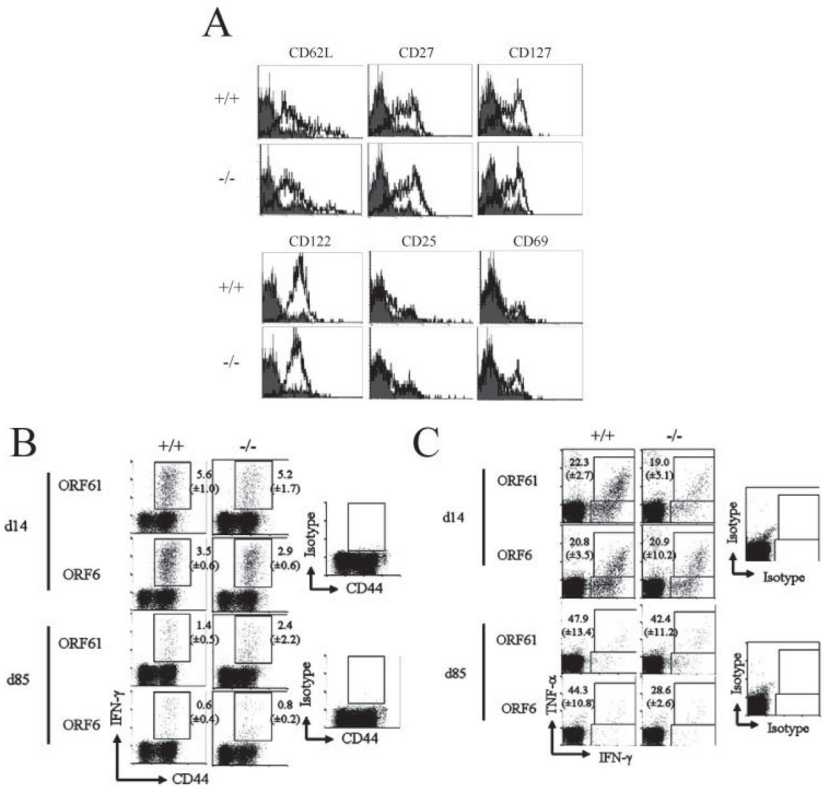

FIGURE 4.

MHV-68-specific $CD8^+$ T cells maintain their cytokine-secreting ability and phenotype in 4-1BBL-deficient mice. *A*, Phenotype of $ORF61_{524–531}/K^b$-specific $CD8^+$ T cells at 86 days postinfection. Representative data plots gated on $CD8^+$tetramer$^+$ cells are shown. Shaded histograms, Isotype control; bold lines, Ab indicated above plots. IFN-γ (*B*) or TNF-α (*C*) production by virus-specific $CD8^+$ T cells at days 14 and 85 postinfection was measured by intracellular cytokine staining. *B*, Representative data plots gated on $CD8^+$ cells are shown. Numbers indicate average percent of $CD8^+$ T cells secreting IFN-γ (±SD). *C*, Representative data plots gated on $CD8^+$ cells are shown. Numbers indicate percent of IFN-γ-secreting cells that also secreted TNF-α (±SD). For each figure, representative data from two experiments using three to four mice per group are shown.

Author Manuscript Author Manuscript Author Manuscript Author Manuscript

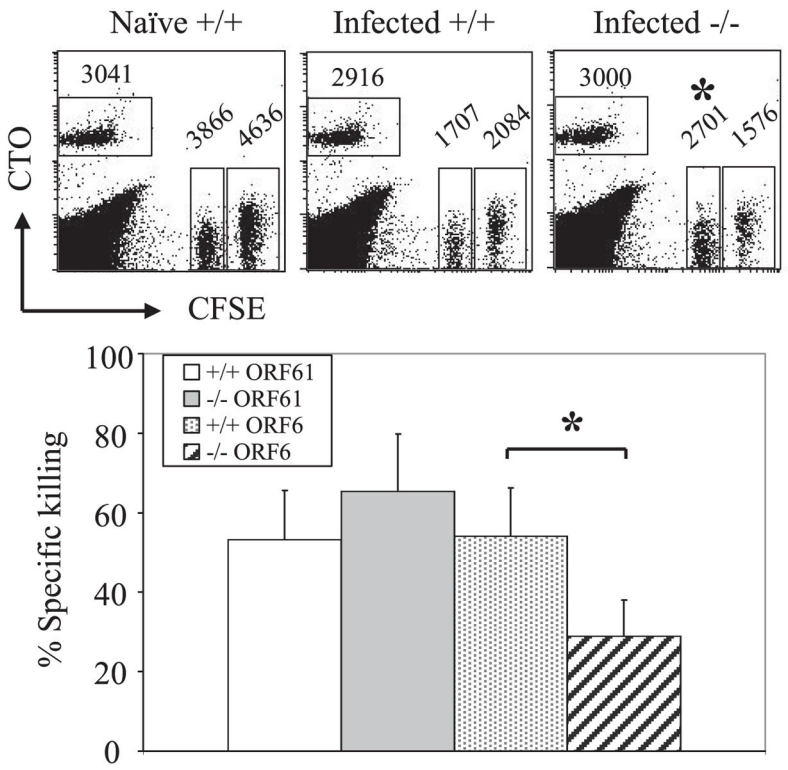

FIGURE 5.

Cytotoxicity by virus-specific $CD8^+$ T cells is decreased during latency in 4-1BBL-deficient mice. Cytotoxicity by virus-specific $CD8^+$ T cells was measured 138 days postinfection by an in vivo CTL assay as described in *Materials and Methods. Top*, Representative data plots from naive B6 (Naive +/+), MHV-68-infected B6 (Infected +/+), or MHV-68-infected 4-1BBL$^{-/-}$ mice (Infected −/−), gated on 7-AAD-negative splenocytes. CTO^{high}, No peptide; CFSE^{high}, $ORF61_{524–531}$ pulsed; CFSE^{low}, $ORF6_{487–495}$ pulsed. Numbers indicate average of total cell numbers in each population (three to four mice per group). *Bottom*, Specific killing was calculated and graphed. Error bars indicated SD. Representative data from two independent experiments are shown.*, $p < 0.05$.

Author Manuscript Author Manuscript Author Manuscript Author Manuscript

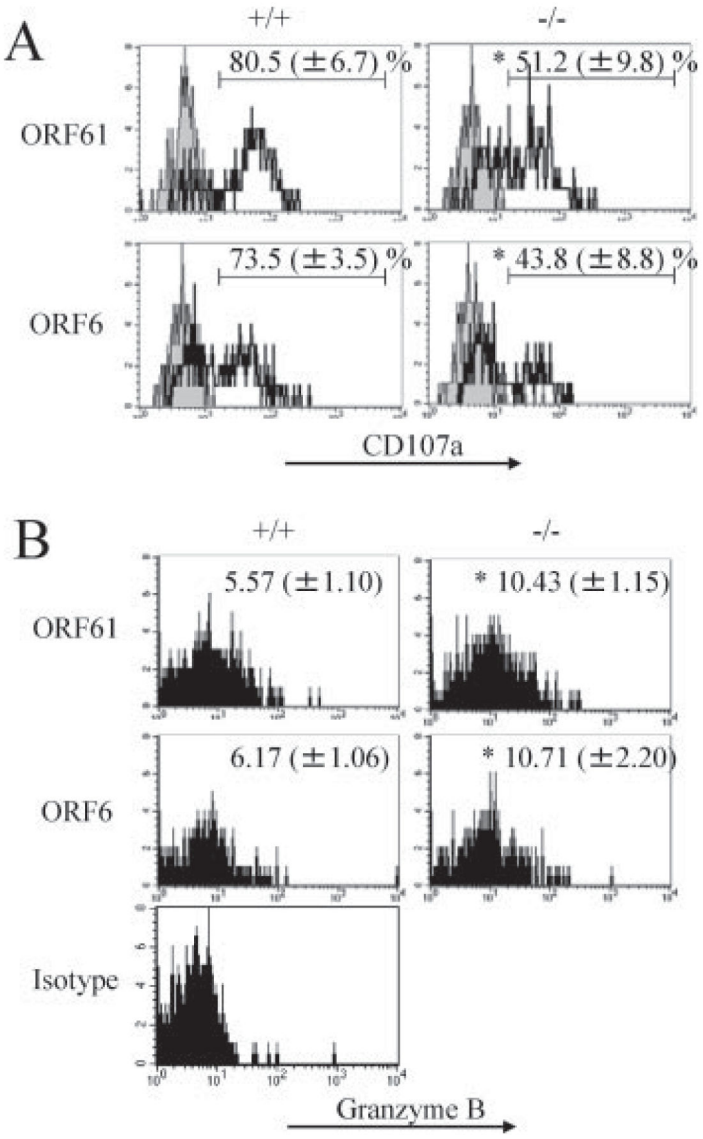

FIGURE 6.

Impaired degranulation by virus-specific $CD8^+$ T cells in the absence of 4-1BBL. *A*, Degranulation by the virus-specific $CD8^+$ T cells at day 85 postinfection were analyzed as described in *Materials and Methods*. Representative data plots gated on $CD8^+$IFN-γ^+ cells are shown. Numbers indicate average percent positive for CD107a (±SD). Shaded histograms, Isotype control; bold lines, anti-CD107a. *B*, Granzyme B expression was examined upon restimulation with indicated peptides in vitro for 5 h. Representative data plots gated on $CD8^+$IFN-γ^+ cells are shown. Numbers indicate mean fluorescence intensity (±SD). Representative data from two experiments using three to four mice per group are shown.*, $p < 0.01$.

Author Manuscript Author Manuscript Author Manuscript Author Manuscript

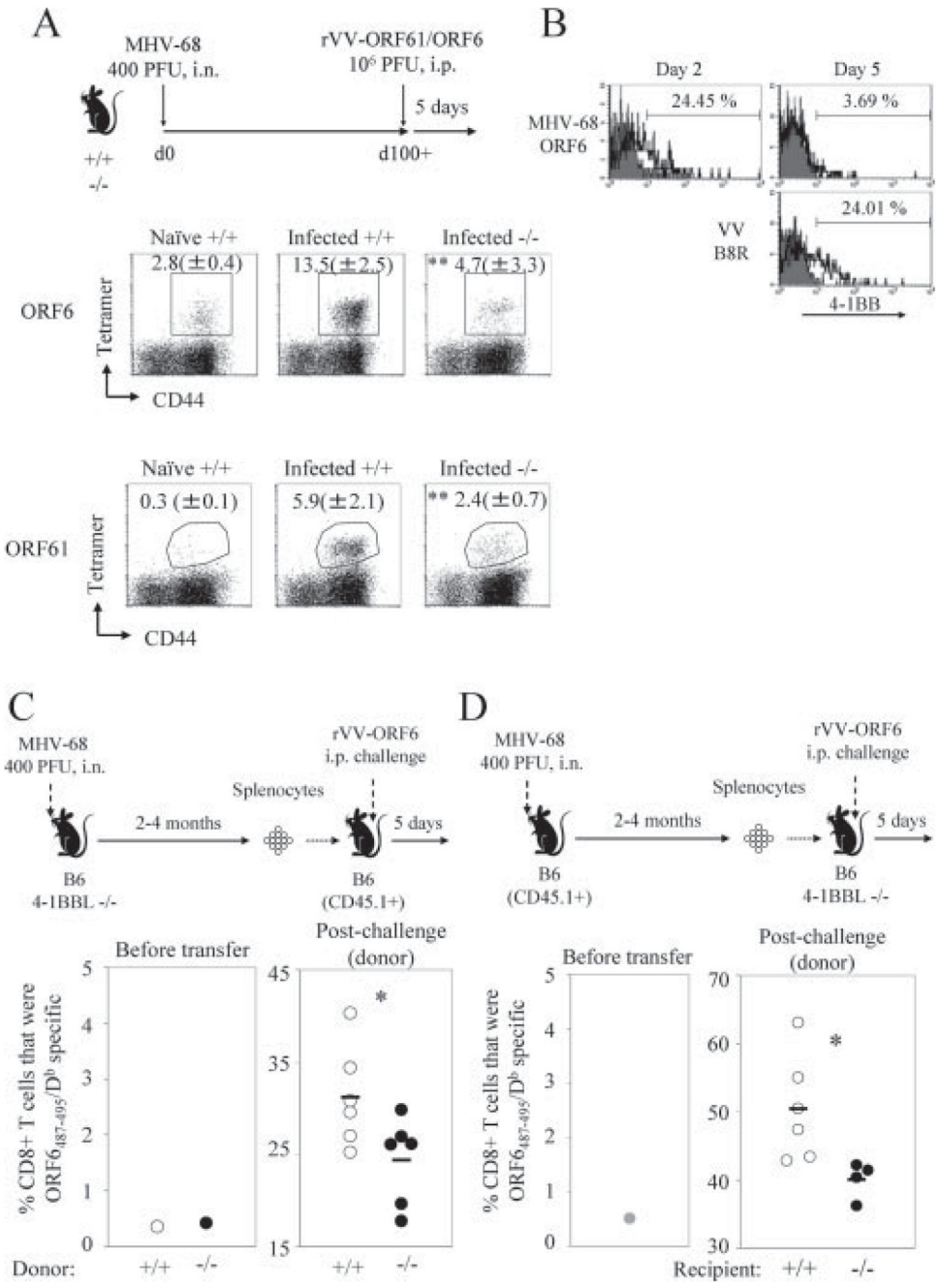

FIGURE 7.

MHV-68-specific memory $CD8^+$ T cells are defective in secondary expansion in the absence of 4-1BBL. *A*, Naive B6 (Naive +/+), MHV-68-infected B6 (Infected +/+), or MHV-68-infected 4-1BBL$^{-/-}$ mice (Infected −/−) were challenged i.p. with 10^6 PFU of rVV-ORF61 or ORF6 at day 100^+ post-MHV-68 infection. Virus-specific $CD8^+$ T cell expansion in the spleen was enumerated at day 5 postchallenge by MHC/peptide tetramer staining. The experimental scheme is indicated above. Plots are gated on $CD8^+$ cells and shown is the average percentage of tetramer$^+$ cells ± SD. **, $p < 0.02$ (Mann-Whitney *U* test, two-tailed).

Author Manuscript Author Manuscript Author Manuscript Author Manuscript

B, Expression of 4-1BB on virus-specific $CD8^+$ T cells specific for the indicated epitopes was analyzed at the indicated days after secondary challenge of infected B6 mice with rVV-ORF6. Representative data gated on $CD8^+$tetramer$^+$ cells are shown. *C*, A total of 2×10^7 splenocytes from MHV-68-infected B6 or 4-1BB$L^{-/-}$ mice 4 mo postinfection were adoptively transferred into naive B6-$CD45.1^+$ recipients. One day posttransfer, mice were challenged with 2.5×10^6 PFU of rVV-ORF6 i.p., and expansion of virus-specific $CD8^+$ T cells was measured by MHC/peptide tetramer staining at 5 days postchallenge. Experimental scheme is shown above, and the percentages of tetramer$^+CD8^+$ T cells among the donor population before and after transfer are graphed below. Each dot represents an individual animal and horizontal bars indicate mean value. *D*, Similar experiments described in *C* were performed, except that $2 ^+ 10^7$ splenocytes from MHV-68-infected B6-CD45.1 plus 2 mo postinfection were adoptively transferred into naive B6 or 4-1BB$L^{-/-}$ mice recipients. Representative data from two to three independent experiments with three to four mice per group are shown. *, $p < 0.05$, Student's *t* test.

Author Manuscript Author Manuscript Author Manuscript Author Manuscript

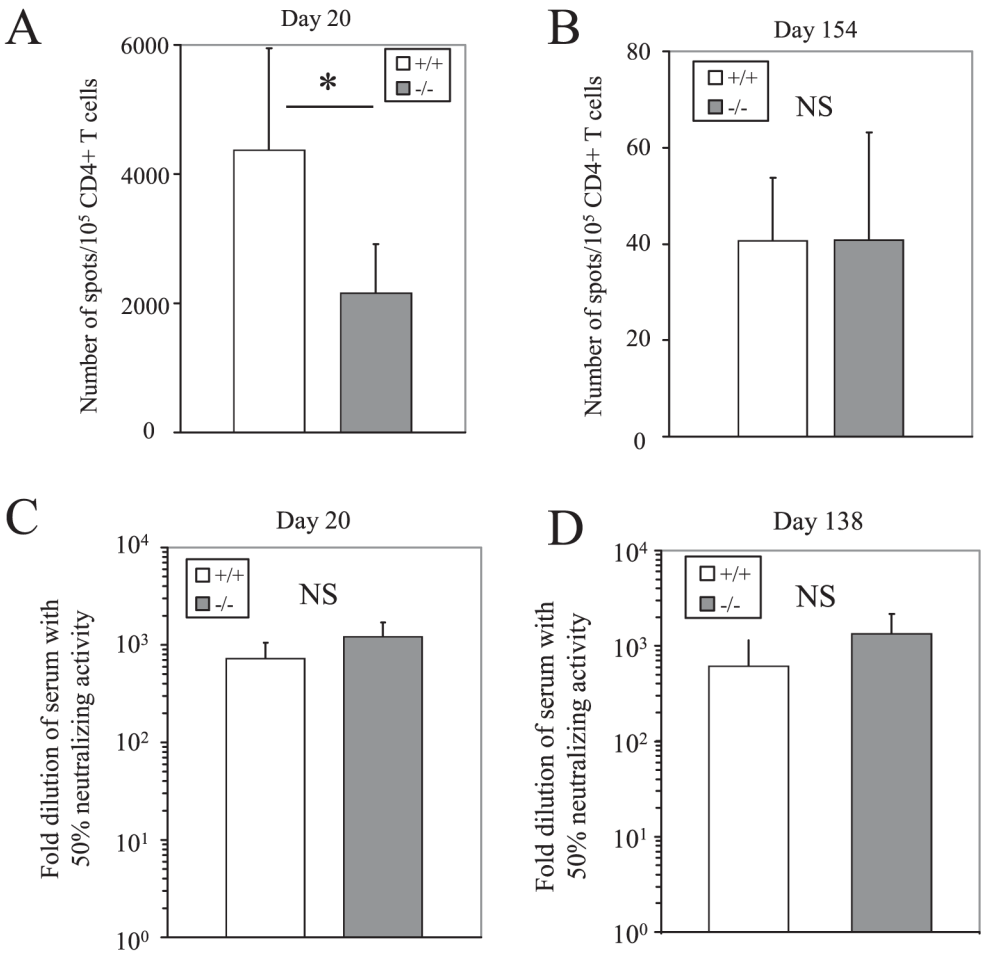

FIGURE 8.

$CD4^+$ T cell and humoral responses to MHV-68 in 4-1BBL$^{-/-}$ mice. *A* and *B*, Virus-specific $CD4^+$ T cell responses were quantified at day 20 (*A*) or day 154 (*B*) postinfection by an ELISPOT assays as described in *Materials and Methods*. Error bars indicate SD. *C* and *D*, Virus-neutralizing activity in the serum at 20 (*C*) or 138 (*D*) days postinfection was assayed by a virus-neutralizing assay. Error bars indicate SD. For each figure, representative data from two experiments using three to six mice per group are shown.*, $p < 0.005$, Student's *t* test.